Fluorine-18-Labeled Progestin 16α,17α-Dioxolanes: Development of High-Affinity Ligands for the Progesterone Receptor with High in Vivo Target Site Selectivity†

Brad O. Buckman,‡ Thomas A. Bonasera,§ Karen S. Kirschbaum,‡ Michael J. Welch,§ and John A. Katzenellenbogen*,‡

Department of Chemistry, University of Illinois, Urbana, Illinois 61801, and Mallinckrodt Institute of Radiology, Washington University Medical School, 510 South Kingshighway, St. Louis, Missouri 63110

Received August 23, 1994®

We describe the synthesis and tissue biodistribution of two 21-[*fluoro*-^{18}F]progestin 16α,17α-furanyl ketals, potential agents for imaging progesterone receptor (PR)-positive breast tumors in humans, using positron emission tomography. 21-Fluoro-16α,17α-[(*R*)-(1′-α-furylmethylidene)dioxy]-19-norpregn-4-ene-3,20-dione (endo-**10a**) and 21-fluoro-16α,17α-[(*R*)-(1′-α-furylethylidene)dioxy]-19-norpregn-4-ene-3,20-dione (endo-**10b**) were chosen for radiochemical synthesis from a series of seven novel progestin 16α,17α-(furanyldioxolanes) on the basis of their high relative binding affinity to PR (190% and 173%, respectively, relative to R5020 = 100%), their low nonspecific binding (NSB) (log $P_{o/w}$ = 3.87 and 4.13, respectively), and their resulting high binding selectivity indices (BSI; i.e., the ratio of their PR binding affinity to nonspecific binding). Radiochemical synthesis of these two species in high radiochemical purity and at high effective specific activity was accomplished by treatment of the corresponding diastereomerically pure 21-trifluoromethanesulfonates with fluorine-18 anion. In tissue biodistribution studies in estrogen-primed immature female Sprague–Dawley rats, both [^{18}F]-endo-**10a** and [^{18}F]endo-**10b** demonstrated high PR-selective uptake in the principal target tissues, the uterus and the ovaries, and relatively low uptake in fat and bone. The metabolism at the 21-position in these progestins (as monitored by in vivo defluorination) appears to be less than that in other 21-fluoroprogestins; this may reflect steric inhibition of metabolism at this site due to the bulk of the furan-substituted dioxolane ring at the 16α,17α-position. Comparison with other fluorine-18-labeled progestins shows that the PR-specific uptake in uterine tissue correlates with the BSI of the ligand and that the fat uptake correlates with the NSB of the ligand at high levels of statistical significance. These two dioxolanes may prove to be useful as breast tumor-imaging agents in humans.

Introduction

The presence of receptors for estrogens and progestins in breast tumors has been used to evaluate tumor aggressiveness and predict the likelihood of responsiveness to hormonal therapy.[1] The prognostic value of these tumor receptor assays has prompted the development of estrogen receptor (ER)- and progesterone receptor (PR)-based imaging agents. Such agents hold the promise of delineating the receptor positivity of tumors in a noninvasive, comprehensive fashion: They might enable an evaluation of the receptor positivity of metastatic tumors and lymph nodes that are inaccessible to surgical or needle biopsy, and they might provide a more accurate prediction of hormonal responsiveness via the in vivo assessment of hormone receptor interaction in situ.

In principle, an imaging agent based on either ER or PR might be used for imaging receptor-positive tumors in an untreated patient. However, there are reasons why a PR-based agent might be preferred to an ER-based one: (1) There is a better correlation between PR positivity and hormonal responsiveness than there is with ER positivity,[1] and (2) a PR-based agent could be used after the initiation of anti-estrogen hormonal therapy, whereas an ER-based agent would not be useful when tumor ER is saturated by the hormonal agent.[2] Moreover, PR-based imaging of breast tumors during the initial course of tamoxifen treatment might be particularly informative in monitoring tumor response: The effectiveness of the hormonal therapy could be signaled initially by enhanced uptake, as the initial agonistic effect of tamoxifen induces PR levels;[3] thereafter, as the antagonistic effect of tamoxifen dominates, tumor regression would be reflected by reduced uptake.

A number of laboratories have demonstrated that estrogens with a variety of different structures, labeled with radioisotopes of fluorine and iodine, retain high ER binding affinity and show good target site-selective uptake in experimental animals in vivo.[4,5] Several of these estrogens have proven to be effective in humans, where clear images of primary and metastatic ER-positive tumors have been observed.[6] The situation with the PR-based agents, however, is less satisfactory. Although they have not been investigated as intensively nor for as long a time, some agents that appear satisfactory in vitro and in experimental animals[7] have given disappointing results in humans.[8] As far as is

† Throughout this paper, the "endo" and "exo" designations refer to the orientation of the aromatic substituent on the dioxolane with respect to the steroid skeleton. Thus, the endo diastereomer has the aromatic substituent positioned underneath the plane of the D-ring. The absolute sterechemistry of the C-2 of the the dioxolane is *R* for the endo isomer and *S* for the exo isomer.

* Address correspondence to John A. Katzenellenbogen, Department of Chemistry, University of Illinois, 461 Roger Adams Laboratory, Box 37, 600 S. Mathews Ave., Urbana, IL 61801. Telephone: (217) 333-6310. FAX: (217) 333-7325. e-mail: katzenel@aries.scs.uiuc.edu.

‡ University of Illinois.

§ Washington University Medical School.

® Abstract published in *Advance ACS Abstracts,* December 1, 1994.

0022-2623/95/1838-0328$09.00/0

Scheme 1

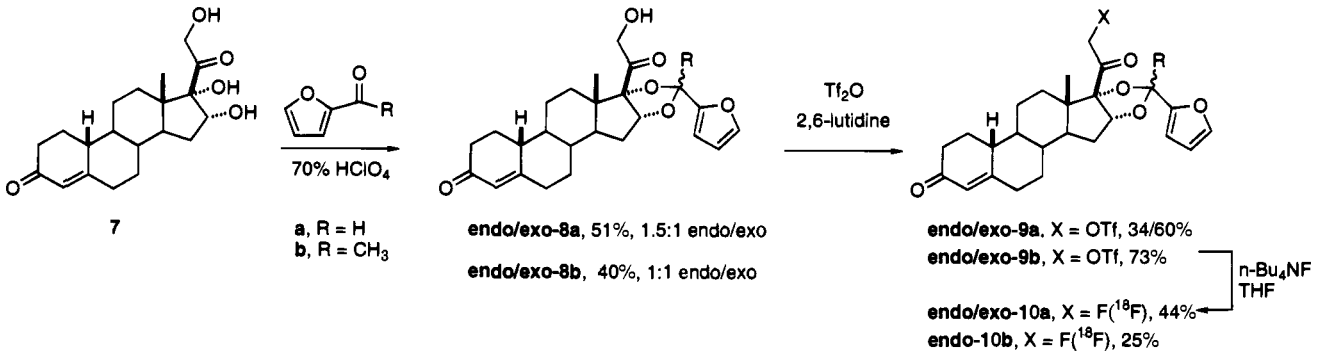

presently understood, there appear to be three sources of these problems: (1) low affinity of these agents for PR, (2) high lipophilicity (which results in high nonreceptor binding), and (3) high metabolic lability.

We[7a] and others[7f,8b] have examined 21-fluoroprogestins (such as **4**) related to the selective, high-affinity progestin ORG 2058 (**3**) and various analogs. However, despite their high PR binding affinity, their moderate nonreceptor binding, and their favorable target tissue-selective uptake in rats, these agents have failed to give satisfactory images of PR-positive tumors in humans. The major problem appears to be a reduction of the C-20 ketone, which occurs rapidly in humans but not in rats, that results in an inactive 20-hydroxy steroid metabolite.[8] Considerable defluorination of these agents also occurred, suggesting that the C-21-position is susceptible to hydroxylation, as well.

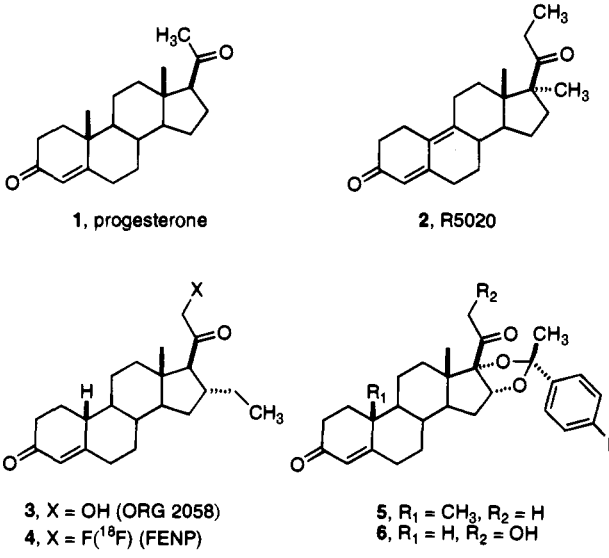

More recently, we have described the preparation of two progestin 16α,17α-dioxolanes, **5** and **6**, that were designed to avoid defluorination by placing the label on the phenyl ring of the acetophenone ketal system.[9] While these agents were rather inert toward metabolic defluorination, their lipophilicity was quite high, and consequently the efficiency and selectivity of their target tissue uptake in vivo were only moderate. The bulk of the 16α,17α-dioxolane system, however, suggested that this structure might be an effective one in moderating the sensitivity of the C-20 ketone to reduction by 20-dehydrogenases.[7g,8b,10] Therefore, we considered what structural modifications might preserve the protective effect offered by this structure toward C-20 reduction while at the same time affording enhanced PR binding affinity and reduced lipophilicity (and hence reduced nonreceptor binding).

In this report, we describe the preparation of a number of progestins (**8a,b, 10a,b**) that embody a 16α,17α-furfural acetal or acetylfuran ketal system, two of which, as C-21 fluorine-18-labeled species, appear to have very favorable characteristics for PR-based imaging: high PR affinity, moderate lipophilicity, and selective in vivo target tissue biodistribution in rats.

Results

Chemical Synthesis of Furanyl 16α,17α-Acetals and -Ketals. The desired compounds are synthesized by ketalizing furfural or 2-acetylfuran with triol **7** under acid catalysis (Scheme 1).[9,11,12] Under our best conditions, a solution of triol **7** in a 0.02 M solution of 70% perchloric acid in furfural afforded a 51% yield of a 1.5:1 mixture of endo/exo-**8a**, whereas triol **7** in a 0.04 M solution of 70% perchloric acid in 2-acetylfuran afforded a 40% yield of a 1:1 mixture of endo/exo-**8b**.

Formation of the dioxolane ring generates a new stereogenic center and affords mixtures of endo and exo diastereomers. In early studies on the formation of progestin 16α,17α-dioxolanes, Fried[12] showed that the diastereomer that was most stable was a function of the structure of the carbonyl component: with aromatic aldehydes, the aryl endo isomer was the more stable, whereas with aromatic methyl ketones, the aryl exo isomer was the more stable. In both cases, the less stable isomer was formed preferentially under conditions of kinetic control (low acid, short times), whereas the more stable one predominated under conditions of thermodynamic control (high acid, longer times). Thus, since the aryl endo isomer is the more biologically active, the preferred conditions for forming the active isomer are thermodynamic for the aldehydes and kinetic for the ketones.

These preferences are pronounced when the aromatic substituent is phenyl, so that acetophenone ketals **5** and **6** can be formed with high selectivity under kinetic control.[9,11,12] In contrast, however, furan acetals **11**[12] and ketals **12**[11a,12] form as mixtures, and triol **7** gives nearly 1:1 mixtures of diastereomers when reacted with furfural and 2-acetylfuran under either thermodynamic or kinetic conditions. Because of the instability of the furan ring to acid, we have optimized the conditions to give the highest yields of **8a,b**, rather than to give mixtures highest in the endo isomers. The pure diastereomers are obtained by semipreparative reversed-phase HPLC, and the stereochemistry of the newly

Table 1. Data for Progestin Ligands

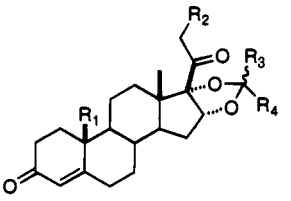

5-13

entry no.	compd no.	R_1	R_2	R_3 (endo)	R_4 (exo)	RBA[a]	log $P_{o/w}$[b]	NSB[c]	BSI[d]
1	progesterone (1)[e]					13	3.87	0.83	16
2	R5020 (**2**)[e]					100	4.05	1.00	100
3	ORG 2058 (**3**)[e]					200	4.02	0.97	206
4	FENP (**4**)[e]					700	4.66	1.87	374
5	**5**	CH_3	H	*p*-C_6H_4F	CH_3	53	5.71	5.52	10
6	**6**	H	OH	*p*-C_6H_4F	CH_3	240	4.92	2.45	98
7	endo-**8a**	H	OH	2-C_4H_3O	H	44	3.78	0.76	58
8	exo-**8a**	H	OH	H	2-C_4H_3O	3	4.01	0.96	3
9	endo-**8b**	H	OH	2-C_4H_3O	CH_3	13	3.90	0.86	15
10	exo-**8b**	H	OH	CH_3	2-C_4H_3O	3	4.23	1.20	3
11	endo-**10a**	H	F	2-C_4H_3O	H	190	3.87	0.83	229
12	exo-**10a**	H	F	H	2-C_4H_3O	11	4.11	1.06	10
13	endo-**10b**	H	F	2-C_4H_3O	CH_3	173	4.13	1.09	159
14	endo-**11**[f]	CH_3	H	2-C_4H_3O	H	18	4.56	1.69	11
15	exo-**11**[f]	CH_3	H	H	2-C_4H_3O	2	4.76	2.08	1
16	endo-**12**[f]	CH_3	H	2-C_4H_3O	CH_3	4	4.76	2.08	2
17	exo-**12**[f]	CH_3	H	CH_3	2-C_4H_3O	1	5.03	2.74	<1
18	**13**[g]	H	F	*p*-C_6H_4F	CH_3	282	5.48	4.36	65

[a] Relative binding affinity at 0 °C determined in a competitive radiometric binding assay, R5020 = 100%; values are the average of two experiments; details are given in the Experimental Section. [b] log of octanol/water partition coefficient, measured by the method of Minick et al. (ref 18). [c] Nonspecific binding, R5020 = 1.00 (see ref 17). [d] Binding selectivity index: ratio of the RBA to NSB, R5020 = 100 (ref 17). [e] Reference 9. [f] See the Experimental Section and refs 11a and 12. [g] Reference 11b.

formed stereogenic center is assigned by an analysis of the ^{1}H NMR of the C-21 protons. In the case of the exo isomer, the C-21 protons are shifted upfield by ≈0.5 ppm with respect to the endo isomer, as a result of shielding by the aromatic ring.[9,11,12] The biological activity and log *P* of the isomers assigned by NMR as endo further supports the assignment of stereochemistry: in all cases, the endo isomer has higher binding affinity to PR and a lower log *P*.

To facilitate the fluorine-18 radiochemical synthesis, the fluorine label should be introduced as late as possible in the synthesis. While electrophilic fluorinating reagents have been used to fluorinate the 21-position of progestins,[13] our need for high specific activity-radiolabeled compounds restricts us to a nucleophilic fluorination strategy using fluoride ion (fluorine-18 is available in high specific activity only as fluoride ion).[14] Nucleophilic displacements at the sterically hindered 21-position of 19-methyl-16α,17α-steroid dioxolanes rarely proceed in excellent yield,[13] yet formation of 21-fluoro steroids has been accomplished via the α-keto 21-sulfonates.[7a,f,8b,15] Treatment of endo-**8a**, exo-**8a**, and endo-**8b** with trifluoromethanesulfonic (triflic) anhydride and 2,6-lutidine in CH_2Cl_2 at −78 °C afforded 21-trifluoromethanesulfinates (triflates) endo-**9a** (34%), exo-**9a** (60%), and endo-**9b** (73%). Displacement of the 21-triflates **9a,b** in the presence of *n*-Bu_4NF in THF at 0 °C gave a 44% yield of a 1:3 mixture of endo/exo-**10a** (derived from a 1:3 mixture of endo/exo-**9a**), while endo-**9b** afforded a 25% yield of endo-**10b**. Separation of endo/exo-**10a** by semipreparative reversed-phase HPLC afforded pure diastereomers.

Progesterone Receptor Binding Affinities (RBA). Competitive radiometric binding assays were used to determine the binding affinities relative to R5020 (**2**) (RBA = 100%).[7c] Historically, we have found that these values are generally reproducible with a coefficient of variation of 0.3. The RBA for both diastereomers of the new ligands **8a,b** and **10a,b** are shown in comparison to the structurally related 16α,17α-ketals **5**, **6**, and **11**−**13** and the other progestins **1**−**4** (Table 1). From these data, it is clear that PR binding affinity in this series of progestins depends on several facets: (a) dioxolane stereochemistry and structure (endo vs exo, phenyl vs furanyl, acetal vs ketal), (b) steroid skeleton (progestin vs 19-nor-21-hydroxyprogestin), and (c) 21-substituent (OH vs F).

Generally, 16α- or 17α-substituents enhance the binding of ligands to the PR,[14] and this new series of 16α,17α-(furanyldioxolanes) (**8** and **10**) shows high affinity for PR. We[9,11] and others[12] have shown that if the 16α,17α-dioxolane aromatic substituent is endo, the PR binding affinity is larger than if the substituent is exo. This is readily seen in the 4−17-fold larger binding affinity of the endo over the exo isomers of **8a,b**, **10a**, **11**, and **12** (cf. Table 1: entries 7 vs 8, 9 vs 10, 11 vs 12, 14 vs 15, and 16 vs 17). Substitution of the *p*-fluorophenyl endo aromatic dioxolane moiety by furan causes a reduction in the RBA of 1.6-fold for the 21-fluoro compounds (**13** vs endo-**10b**; cf. Table 1: entry 18 vs 13), 18.5-fold for the 21-hydroxy compounds (**6** vs endo-**8b**; cf. Table 1: entry 6 vs 9), and 13.3-fold for the 19-methylprogestin compounds (**5** vs endo-**12**; cf. Table 1: entry 5 vs 16). Finally, the furan acetals demonstrate a slightly higher binding affinity than that of the furan ketals, in most cases (cf. Table 1: entries 7 vs 9, 8 vs 10, 11 vs 13, 14 vs 16, and 15 vs 17).

The series of progestins described herein is well suited to illustrating the trend toward higher RBA values when the natural progesterone (**1**) skeleton (ketals **5**,

endo-**11**, endo-**12**) is changed to the 19-nor-21-hydroxy system (ketals **6**, endo-**8a**, endo-**8b**). In the dioxolane series, changing from the progesterone skeleton to the 19-nor-21-hydroxy system causes an average 3-fold increase in binding affinity (cf. Table 1: entries 5 vs 6, 14 vs 7, and 16 vs 9).

The dioxolane compounds derived from the 19-nor-21-hydroxyprogestin skeleton (ketals **6**, endo-**8a**, endo-**8b**; Table 1: entries 6, 7, and 9) show binding affinity that is equal to or higher than progesterone itself. However, if a 21-fluoro substituent is introduced, the binding affinities are greatly enhanced (RBA endo-**10a** = 190%, endo-**10b** = 173%, **13** = 282%; cf. Table 1: entries 11, 13, and 18). In the furanyl acetal endo-**8a** and furan ketal endo-**8b**, 21-fluoro for 21-hydroxyl substitution results in a 4.3- and 13-fold increase, respectively (cf. Table 1: entries 7 vs 11 and 9 vs 13); however, in the *p*-fluoroacetophenone ketal system **6**, 21-fluoro for hydroxyl substitution results in only a 1.2-fold increase (cf. Table 1: entries 6 vs 18). In a different system, 21-fluoro for hydroxyl substitution results in a 3.5-fold increase in binding affinity of FENP (**4**) over the corresponding 21-hydroxy-substituted ORG 2058 (**3**) (cf. Table 1: entries 4 vs 3). Thus, the magnitude of this change depends on the structure of the steroid skeleton.

Octanol/Water Partition Coefficient Determination. The lipophilicity of a steroidal ligand can be predictive of its binding to low-affinity, nonspecific sites.[17] To estimate the lipophilicity of the 16α,17α-dioxolane ligands, the octanol/water partition coefficients (log $P_{o/w}$) were measured using a reversed-phase HPLC method (Table 1).[18] We have previously used this method to measure the lipophilicities of other substituted estrogens and progestins.[5,9,11] Structures incorporating the 19-nor-21-hydroxyprogestin skeleton not only benefit from higher RBA than natural progestin analogs (as described above) but also benefit from reduced lipophilicity resulting from the elimination of the lipophilic 19-methyl group and addition of a hydrophilic 21-hydroxyl group. The lower lipophilicity is seen in the 6–8-fold decrease in $P_{o/w}$ when comparing acetophenone ketals **5** and **6**, furan acetals endo-**8a** and endo-**11**, and furan ketals endo-**8b** and endo-**12**, respectively (Table 1: entries 5 and 6, 7 and 14, 9 and 16). Most importantly, changing the aromatic substituent from a *p*-fluorophenyl ring to a furan ring dramatically decreases the lipophilicity, 22.4-fold in **13** to endo-**10b** (Table 1: entries 18 vs 13) and 10.5-fold in **6** to endo-**8b** (Table 1: entries 6 vs 9). An effect of this magnitude was anticipated, since the $P_{o/w}$ of fluorobenzene is 8.5-fold higher than furan.[19]

The increased binding affinity of furan acetal ligand **10a** and furan ketal ligand **10b** that results from the replacement of the 21-hydroxyl substituent with fluorine atom is also accompanied by an increase in the lipophilicity. However, this substitution causes only a 1.2- and 1.7-fold increase in $P_{o/w}$, respectively (Table 1: entries 7 vs 11 and 9 vs 13), whereas the same substitution in the acetophenone ketals **3** and **6** causes a 4.4- and 3.6-fold increase in $P_{o/w}$, respectively (Table 1: entries 3 vs 4 and 6 vs 18). Thus, it appears that the furan for phenyl substitution tempers the effect of the increased lipophilicity of the 21-fluorine for 21-hydroxy substitution.

Estimation of Nonspecific Binding and Binding Selectivity Indices. We have shown that the nonspecific binding affinity (NSB) of a substituted estrogen can be estimated relative to estradiol on the basis of the difference in their log $P_{o/w}$ values.[5,17] Analogously, the NSB for new progestins can be estimated relative to R5020, which is given the NSB value of 1 (Table 1: entry 3). With a variety of substituted estrogens, the value of the binding selectivity index (BSI) (the ratio of their RBA to NSB) has been correlated with their selectivity and efficiency of uterine uptake.[5] The BSI has been shown to be a better predictor of uterine uptake selectivity than the RBA of the ligand itself. The calculated values for the NSB and BSI are given in Table 1, and these values are used later in correlations with tissue uptake data.

It is noteworthy that substitution of the C-21 OH with an F has two noncomplementary effects on BSI: it increases the RBA, but it also increases the lipophilicity (and consequently nonspecific binding). In furan acetal endo-**10a** and furan ketal endo-**10b**, the 21-F for 21-OH substitution increased the RBA more than we had expected and the increase in lipophilicity was less than noted in the acetophenone series. As a result, endo-**10a** and endo-**10b** possess a much higher BSI than previously prepared ketals **5** and **6**. On this basis, the 21-fluoro furan acetal endo-**10a** and ketal endo-**10b** appeared to be viable candidates for diagnostic imaging agents for the PR, and both were prepared in fluorine-18-radiolabeled form to determine their in vivo biodistribution in rats.

Radiochemical Synthesis. The fluorine-18-labeled furan acetal [^{18}F]endo-**10a** and ketal [^{18}F]endo-**10b** were prepared from the diastereomerically pure 21-triflates endo-**9a** and endo-**9b** by treatment with [^{18}F]Bu_4NF in THF at 25 °C for 5–7 min. During the normal phase semipreparative HPLC purification, which follows the incorporation of the fluorine-18 label, the unreacted triflate elutes just ahead of the desired fluorine-18-labeled products. In such a situation, any triflate or its hydrolysis product (21-hydroxy compound) that may tail from the preceeding peak could coelute with the fluorine-18-labeled species, thus lowering the effective specific activity of [^{18}F]endo-**10a** and [^{18}F]endo-**10b**. To minimize such problems, we adapted the prehydrolysis method used by Pomper in the synthesis of [^{18}F]FENP (**4**).[7a] Thus, 2.5 equiv of *n*-Bu_4NOH was added to the reaction mixture following the incorporation of fluorine-18 but prior to its purification by HPLC. This base hydrolyzes remaining unreacted triflate starting material, giving more polar products that elute after the radiolabeled products. This results in a purer product, although it decreases the yield of isolated product by ≈50%. In this manner, decay-corrected radiochemical yield ranges of 2–13% were obtained for furan acetal [^{18}F]endo-**10a** and 3–8% for furan ketal [^{18}F]endo-**10b**, in a total synthesis time of less than 2 h, with effective specific activities[20] greater than 1200 Ci/mmol. The radiochemical purity of the labeled progestins as determined by reversed-phase HPLC was greater than 95% in all cases.

In Vivo Tissue Biodistributions of [^{18}F]endo-10a and [^{18}F]endo-10b. HPLC-purified furan acetal [^{18}F]-endo-**10a** and ketal [^{18}F]endo-**10b** were dissolved in 10% ethanol–saline and injected (iv, tail vein) into estrogen-primed immature female Sprague–Dawley rats (25 days old, ≈50 g, five rats per time point). Doses employed were 70 μCi/rat for [^{18}F]endo-**10a** and 60 μCi/rat for [^{18}F]-

Table 2. Tissue Biodistribution of Furan Acetal [^{18}F]endo-**10a** into Estrogen-Primed Immature Female Rats[a]

	percent injected dose/g ± SD,[b] $n = 5$			
	1 h	1 h low	1 h blocked	3 h
uterus	6.80 ± 1.70	5.18 ± 2.00	1.68 ± 0.37	7.83 ± 1.41
ovaries	2.76 ± 0.35	2.13 ± 0.60	1.65 ± 0.33	2.62 ± 0.31
blood	0.38 ± 0.08	0.35 ± 0.10	0.46 ± 0.08	0.19 ± 0.07
muscle	0.59 ± 0.08	0.41 ± 0.13	0.71 ± 0.10	0.26 ± 0.08
lung	2.38 ± 0.38	1.51 ± 0.52	1.16 ± 0.25	0.31 ± 0.09
brain	0.57 ± 0.06	0.40 ± 0.11	0.49 ± 0.12	0.18 ± 0.05
liver	2.40 ± 0.18	1.81 ± 0.51	2.49 ± 0.17	1.65 ± 0.25
kidney	1.66 ± 0.32	1.14 ± 0.25	1.72 ± 0.36	0.73 ± 0.26
fat	2.16 ± 0.71	2.15 ± 0.60	2.40 ± 0.78	2.36 ± 0.52
bone	1.11 ± 0.20	0.99 ± 0.31	1.29 ± 0.15	1.30 ± 0.45
uterus/blood	18.18 ± 4.85	14.95 ± 3.28	3.68 ± 0.65	47.99 ± 24.36
uterus/muscle	11.63 ± 3.34	12.85 ± 3.36	2.34 ± 0.27	32.23 ± 10.95

[a] See the Experimental Section for details. [b] SD is standard deviation.

Table 3. Tissue Biodistribution of Furan Ketal [^{18}F]endo-**10b** into Estrogen-Primed Immature Female Rats[a]

	percent injected dose/g ± SD,[b] $n = 5$			
	1 h	1 h low	1 h blocked	3 h
uterus	6.51 ± 2.30	3.46 ± 0.87	1.43 ± 0.29	8.65 ± 2.73
ovaries	3.04 ± 0.33	1.58 ± 0.61	1.52 ± 0.58	2.66 ± 0.44
blood	0.32 ± 0.08	0.35 ± 0.08	0.60 ±0.18	0.14 ± 0.06
muscle	0.64 ± 0.36	0.25 ± 0.13	0.54 ± 0.09	0.20 ± 0.10
lung	1.92 ± 0.54	1.23 ± 0.48	1.16 ± 0.29	0.27 ± 0.05
brain	0.58 ± 0.08	0.34 ± 0.10	0.49 ± 0.13	0.19 ± 0.04
liver	1.26 ± 0.29	0.68 ± 0.42	1.52 ± 0.72	1.61 ± 0.22
kidney	1.59 ± 0.44	0.97 ± 0.38	1.84 ± 0.38	0.76 ± 0.29
fat	2.86 ± 1.44	1.86 ± 1.81	3.48 ± 1.37	4.16 ± 1.38
bone	1.15 ± 0.39	0.84 ± 0.33	1.29 ± 0.43	1.51 ± 0.66
uterus/blood	20.09 ± 3.82	10.00 ± 1.51	2.47 ± 0.57	71.09 ± 37.73
uterus/muscle	12.07 ± 7.44	12.09± 1.92	2.68 ± 0.56	53.06 ± 31.00

[a] See the Experimental Section for details. [b]SD is standard deviation.

endo-**10b**. Tissue biodistributions of fluorine-18 radioactivity were determined at 1 and 3 h postinjection (Tables 2 and 3). To determine whether the uptake was mediated by a high-affinity, limited-capacity system, one set of animals was coinjected with the fluorine-18-labeled progestin together with 18 μg of ORG 2058 in order to fully occupy the progesterone receptors (Table 2 and 3, 1 h "blocked"). To establish that the uptake was not being limited by undetected PR-binding impurities, one set of animals was injected with only 20% of the 1 h dose (Tables 2 and 3, 1 h "low dose").

The tissue biodistribution data for furan acetal [^{18}F]-**endo10a** and furan ketal [^{18}F]**endo10b** at 1 h postinjection show high uptake in the uterus and ovaries, which are the target organs containing PR. Receptor-mediated uptake is indicated by the decreased uptake in the uterus and ovaries of the blocked animals: 75–80% less uptake in uterus and 40–50% less uptake in ovaries for [^{18}F]endo-**10a** and [^{18}F]endo-**10b**. As expected from the high measured effective specific activities of these compounds, the target tissue uptake in the low-dose animals was not higher than in the regular dose series. The uterine uptake is prolonged, and it continues to rise from 1 to 3 h. For both compounds, considerable clearance of activity from the blood, muscle, liver, lung, kidney, and brain from 1 to 3 h is observed. As a result, the ratios of uterine uptake to muscle and uterine uptake to blood increase significantly from 1 to 3 h.

The extent of in vivo defluorination of these compounds is relatively modest, indicated by bone activity at 3 h of 1.30% and 1.51% ID/g for compounds [^{18}F]endo-**10a** and [^{18}F]endo-**10b**, respectively. (These levels correspond to % ID/organ values of 7.49 and 8.90.) Also of note are the relatively low levels of liver and fat uptake. While liver activity drops over the 1–3 h period, bone and fat levels remain relatively constant.

Discussion

We have described, in the present study and in earlier work,[9] the synthesis of four progestin 16α,17α-dioxolanes in fluorine-18 labeled-form (**5**, **6**, endo-**10a**, and endo-**10b**) and have shown that they bind to PR with high affinity and show efficient and selective target tissue uptake in rats. Our interest in the 16α,17α-dioxolanes was stimulated by our desire to obtain PR-based imaging agents that would not suffer from the rapid metabolism encountered by our first fluorine-18-labeled progestin, FENP (**4**), when used in humans: This radiopharmaceutical appeared to be very well behaved on the basis of in vitro binding and tissue distribution studies in rats,[7a] but in humans it failed to provide satisfactory images in PR-positive breast tumors.[8a] Our further studies of FENP metabolism in rat hepatocyte cultures indicated considerable generation of nonpolar metabolites.[8a,21] Subsequent studies by Vaalburg indicated that this was the 20-hydroxy steroid, a common metabolite of pregnandione steroids.[8b]

Early reports by Fried documented that the addition of a 16α,17α-dioxolane system into the pregnenedione system produced compounds that were potent progestins.[12] These, together with other progestin derivatives having bulky substituents at the 16α- and 17α-positions,[9,11] confirmed that PR is tolerant to substituents projecting behind the D-ring. We surmised that bulky dioxolanes might protect the steroid from 20-dehydrogenases, and in our initial work in this series, we prepared two progestins substituted with fluorine within the acetophenone unit of the ketal (**5**, **6**).[9] The preparation of these compounds labeled with fluorine-18 was a challenge, as it involved a nucleophilic aromatic displacement reaction to introduce the radiolabel into the acetophenone followed by a rapid ketalization under demanding conditions to attach the *p*-fluoroacetophenone to the steroid. The resulting steroids were also rather lipophilic, a characteristic that compromised to some extent the selectivity of their in vivo distribution.

The corresponding furanyl ketals and acetals (Table 1: entries 14–17) were also described in the initial reports of the 16α,17α-dioxolanes,[12] and these offered the possibility of reduced lipophilicity compared to the acetophenone ketals. This hydrophilizing change from phenyl to furan was to be coupled with radiolabeling at the C-21-position by replacing the C-21 hydroxyl with the fluorine-18, a substitution that elevates lipophilicity but has in the past resulted in a marked elevation of binding affinity. The result was the two compounds [^{18}F]-endo-**10a** and [^{18}F]endo-**10b** described here.

Comparison of PR-Based Affinity Ligands in Vitro and in Vivo. It is instructive to compare furan acetal [^{18}F]endo-**10a** and furan ketal [^{18}F]endo-**10b** with the previously reported acetophenone ketals **5** and **6** and FENP (**4**) in terms of their in vivo tissue biodistribution (Table 4 and Figure 1) and its relation to the BSI and NSB, which are calculated from in vitro measurements of RBA and log $P_{o/w}$ (Table 1). While the ovarian uptake at 1 h postinjection is nearly the same for all five

Table 4. Tissue Biodistribution Comparison for Labeled Progestins in Immature Rats

	percent injected dose/g ± SD[a] at 1 h				
	FENP (**4**)[b]	**5**[c]	**6**[c]	endo-**10a**[d]	endo-**10b**[e]
uterus	6.43 ± 1.53	3.08 ± 0.43	3.65 ± 1.11	6.80 ± 1.70	6.51 ± 2.30
ovaries	2.86 ± 0.78	3.93 ± 0.77	2.80 ± 0.70	2.76 ± 0.35	3.04 ± 0.33
blood	0.25 ± 0.07	0.47 ± 0.04	0.26 ± 0.02	0.38 ± 0.08	0.32 ± 0.08
muscle	0.42 ± 0.10	0.82 ± 0.15	0.44 ± 0.04	0.59 ± 0.08	0.64 ± 0.36
lung	0.47 ± 0.20	1.30 ± 0.35	0.60 ± 0.08	2.38 ± 0.38	1.92 ± 0.54
brain	0.63 ± 0.16	0.56 ± 0.03	0.34 ± 0.05	0.57 ± 0.06	0.58 ± 0.08
liver	3.34 ± 0.90	3.41 ± 0.26	4.25 ± 0.39	2.40 ± 0.18	1.26 ± 0.29
kidney	1.05 ± 0.22	2.18 ± 0.12	1.42 ± 0.08	1.66 ± 0.32	1.59 ± 0.44
fat	3.56 ± 0.66	5.76 ± 1.35	3.53 ± 1.05	2.16 ± 0.71	2.86 ± 1.44
bone	3.18 ± 0.76	1.76 ± 0.48	0.62 ± 0.08	1.11 ± 0.20	1.15 ± 0.39
uterus/blood	26.26 ± 6.58	6.59 ± 0.68	14.00 ± 4.20	18.18 ± 4.85	20.09 ± 3.82
uterus/muscle	15.98 ± 5.51	3.85 ± 0.74	8.20 ± 2.50	11.63 ± 3.34	12.07 ± 7.44

[a] SD is standard deviation. [b] From ref 7a. [c] From ref 9. [d] From Table 2. [e] From Table 3.

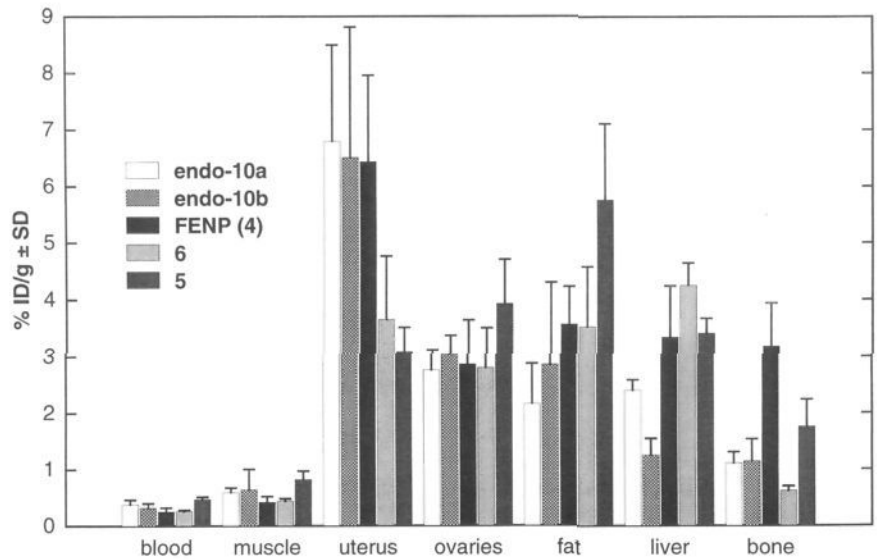

Figure 1. Comparison of tissue biodistribution data of fluorine-18-labeled progestins (from Table 4).

compounds, for [^{18}F]endo-**10a** and [^{18}F]endo-**10b** the blood and muscle uptake is slightly elevated but the liver uptake is significantly decreased. However, with regard to the design goals chosen for the newest generation of imaging ligands, endo-**10a** and endo-**10b** described above, a comparison of the uptake in the uterus, fat, and bone is the most informative.

Due to their high BSI, the high uterine uptake and uterus to non-target-tissue ratios for both [^{18}F]endo-**10a** and [^{18}F]endo-**10b** are comparable to the uptake seen with FENP (**4**) and higher than those of *p*-fluoroacetophenone ketals **5** or **6** (Table 4 and Figure 1). In the past, we have sought to find correlations between the in vitro binding characteristics and in vivo uptake properties of fluorinated estrogen radiopharmaceuticals by comparing in vivo tissue-specific uptake, defined as the difference in uptake between experiments conducted in the absence (total uptake) and presence (nonspecific uptake) of a blocking dose of unlabeled steroid, to the BSI, RBA, or NSB values.[5] Out of all of the possible correlations between either % ID/g of total tissue uptake at 1 h or tissue-specific uptake and the BSI, NSB, or RBA values of these five fluorine-18-labeled progestins, only the uterus, ovaries, fat, and brain show statistically valid correlations ($r^2 > 0.80$; data not shown). In the progestin series discussed here, Figure 2A indicates that there is a good correlation between the BSI value and the specific uptake for the five radiolabeled progestins **4**, **5**, **6**, endo-**10a**, and endo-**10b** in the principal target organ, uterus ($r^2 = 0.85$). As a predictor of uterine-specific uptake, the BSI value is more accurate than are the NSB and RBA values ($r^2 = 0.68$ and 0.45, respectively; not shown).

Since [^{18}F]endo-**10a** and [^{18}F]endo-**10b** have the lowest log *P* and NSB values of the five fluorine-18 progestins described, they also show the lowest total fat uptake at 1 h. The correlation between total fat uptake and the NSB of the five progestins (Figure 2B) also shows a very good correlation ($r^2 = 0.96$).

A good correlation also exists between ovary uptake at 1 h and the NSB of the five labeled progestins ($r^2 = 0.81$; not shown). This is most probably due to the higher fat content of ovaries compared to uterine tissue, causing high uptake due to nonspecific binding to fat.[9] The BSI and RBA values show good correlation to brain specific uptake as well ($r^2 = 0.73$ and 0.93, respectively; not shown). Most all of the other possible correlations are much less statistically significant ($r^2 < 0.6$).

One of the most significant characteristics of the tissue distributions of [^{18}F]endo-**10a** and [^{18}F]endo-**10b** is that they retain their high uterine-specific uptake without the high bone, liver, and fat uptake seen with FENP (**4**). Although endo-**10a** and endo-**10b** possess a fluorine atom in the 21-position analogous to FENP, the activity levels observed in the bone after 1 h are nearly as low as those attained from metabolism of an aromatic fluoride as in the *p*-fluoroacetophenones **5** or **6**, in which the site of fluorine substitution was chosen to be

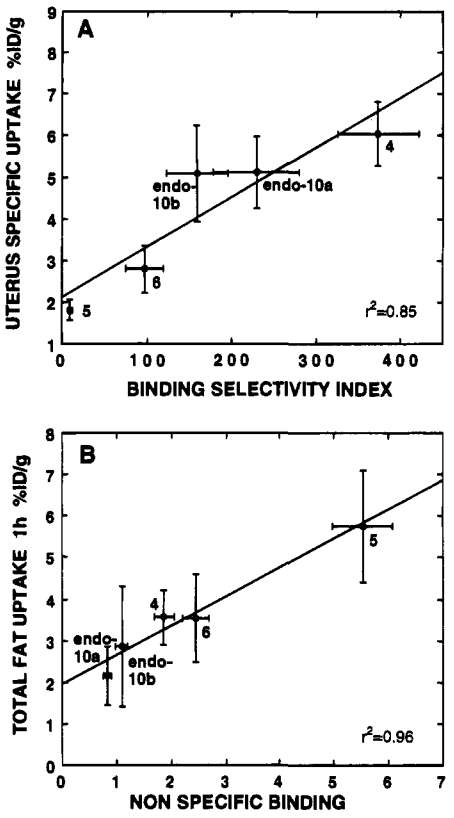

Figure 2. Correlation between PR-specific uterine uptake and BSI and correlation between fat uptake and NSB of five fluorine-18-labeled progestins at 1 h. Specific uptake was calculated as the difference between the uptake in the absence and presence of a blocking dose of ORG 2058 (**3**). The errors in each determination were propagated by standard methods (root mean square values) and are expressed as the standard errors of the mean. The errors in the BSI values are estimated from historical coefficients of variation, being 0.3 and 0.1, respectively, for the RBA and NSB values, giving a propagated coefficient of variation of 0.32.

aromatic, specifically, to reduce in vivo defluorination. The decreased metabolism at the 21-position may be due to the increased steric bulk at the 16α,17α-position derived from the furan-substituted dioxolane ring. This change in metabolism at C-21 suggests that there may be a corresponding reduction in 20-hydroxysteroid dehydrogenase sensitivity of the 16α,17α-dioxolane progestins, a factor that may prove critical for the successful use of these compounds as tumor-imaging agents in humans.

In conclusion, the success in the design of furan acetal endo-**10a** and furan ketal endo-**10b** as high-affinity ligands in vivo for the progesterone receptor involves the choice of 16α,17α-(furanyldioxolane)- and 21-fluoro-substituted progestins. This rationale results in compounds that can be prepared by a facile radiochemical synthesis in high effective specific activity-radiolabeled form from diastereomerically pure 21-triflates endo-**9a** and endo-**9b**. These compounds display low lipophilicity coupled with high binding affinity, giving comensurately high BSI values which are not unbalanced by an inordinately high NSB or RBA. Furthermore, these compounds possess the 16α,17α-steric bulk which decreases their in vivo metabolic defluorination in rats and may decrease the in vivo metabolism by 20-hydroxysteroid dehydrogenase, a metabolic conversion in humans that results in the rapid generation of lipophilic metabolites from FENP. Further studies are underway to determine the extent of blood metabolism of furan acetal endo-**10a** and furan ketal endo-**10b**. If the behavior of these compounds in humans mirrors their behavior in rats, then they may hold promise for the selective in vivo imaging of PR-positive tumors of the breast by positron emission tomography.

Experimental Section

General Methods. Proton, fluorine-19, and carbon-13 magnetic resonance spectra were obtained on a Varian Unity 400 spectrometer at 400, 376, and 101 MHz, respectively. ^{1}H NMR and ^{13}C NMR chemical shifts are reported in ppm downfield from internal tetramethylsilane (δ scale). ^{19}F NMR chemical shifts are reported in ppm upfield from internal $CFCl_3$ (ϕ scale). The data are reported in the form (if applicable): chemical shift (multiplicity, coupling constant, number of protons, assignment). All J values are in hertz (Hz). High-resolution exact mass determinations were obtained on a VG 70-VSE mass spectrometer. Preparative HPLC was performed isocratically using a Whatman ODS-3 partisil 5 RAC (9.4 × 100 mm) reversed-phase column. A standard method for product isolation was used; it involved an aqueous quench and organic extraction, drying of the extract, and removal of solvent in vacuo. Purification was by flash chromatography.[22] Furan acetal endo/exo-**11** and furan ketal endo/exo-**12** were prepared according to literature methods.[11a,12] Triol **7** was prepared by us previously.[9]

16α,17α-[(*R*)-(1′-α-Furylmethylidene)dioxy]-21-hydroxy-19-norpregn-4-ene-3,20-dione (endo-8a) and 16α,17α-[(*S*)-(1′-β-Furylmethylidene)dioxy]-21-hydroxy-19-norpregn-4-ene-3,20-dione (exo-8a). Triol **7** (100 mg, 0.287 mmol) was stirred in a 0.023 M solution of perchloric acid in furfural (6.6 μL of 70% perchloric acid in 3.3 mL of furfural) for 24 h. Product isolation followed by flash chromatography (2:1 hexanes/EtOAc) afforded 64 mg (51%) of a 1.5:1 mixture of endo-**8a** and exo-**8a**. Semipreparative HPLC (70/30 water/CH_3-CN, 5 mL/min) afforded analytical samples for characterization and binding affinity measurements.

Data for endo-8a: ^{1}H NMR δ 7.47 (d, 1, J = 2), 6.52 (d, 1, J = 4), 6.39 (d, 1, J = 3), 5.85 (br s, 1, H-4), 5.59 (s, 1, acetal H), 5.08 (d, 1, J = 5.6, H-16), 4.49 (AB q, 2, $\Delta\nu$ = 0.35 ppm, J = 20, H-21), 0.73 (s, 3, 18-CH_3); ^{13}C NMR δ 210.0, 199.8, 165.8, 143.8, 124.8, 110.3, 110.2, 98.0, 97.9, 82.9, 67.4, 48.7, 47.9, 47.1, 42.3, 39.5, 36.5, 35.3, 33.2, 31.4, 31.1, 26.5, 25.6, 14.9; IR ($CHCl_3$) 1740, 1670, 1100 cm^{-1}; mp 165–166 °C; HPLC t_R 32 min; HRMS (CI, M + H) calcd for $C_{25}H_{31}O_6$ 427.2121, found 427.2115. Anal. ($C_{25}H_{30}O_6 \cdot {}^1/_2H_2O$) C, H.

Data for exo-8a: ^{1}H NMR δ 7.39 (br s, 1), 6.33–6.31 (m, 2), 6.19 (s, 1, acetal H), 5.85 (s, 1, H-4), 5.33 (d, 1, J = 6, H-16), 4.15 (AB q, 2, $\Delta\nu$ = 0.12 ppm, J = 20, H-21), 0.74 (s, 3, 18-CH_3); ^{13}C NMR δ 209.5, 199.7, 165.6, 150.3, 143.3, 124.8, 110.3, 109.6, 100.1, 97.9, 84.3, 67.2, 49.3, 48.8, 47.8, 42.3, 39.7, 36.5, 35.3, 33.2, 31.5, 31.1, 26.5, 25.7, 15.1; IR ($CHCl_3$) 1740, 1670, 1100 cm^{-1}; mp 184–185 °C; HPLC t_R 40 min; HRMS (CI, M + H) calcd for $C_{25}H_{31}O_6$ 427.2121, found 427.2114.

16α,17α-[(*R*)-(1′-α-Furylethylidene)dioxy]-21-hydroxy-19-norpregn-4-ene-3,20-dione (endo-8b) and 16α,17α-[(*S*)-(1′-β-Furylethylidene)dioxy]-21-hydroxy-19-norpregn-4-ene-3,20-dione (exo-8b). Triol **7** (115 mg, 3.3 mmol) was stirred in a 0.042 M solution of perchloric acid in 2-acetylfuran (20 μL of 70% perchloric acid in 5.5 mL of 2-acetylfuran) for 2 h. Product isolation followed by flash chromatography (2:1 hexanes/EtOAc) afforded 58 mg (40%) of a 1:1 mixture of endo-**8b** and exo-**8a**. Semipreparative HPLC (70/30 water/CH_3CN, 5 mL/min) afforded analytical samples for characterization and binding affinity measurements.

Data for endo-8b: ^{1}H NMR δ 7.42 (d, 1, J = 2), 6.42 (d, 1, J = 3), 6.36 (d, 1, J = 3), 5.85 (br s, 1, H-4), 5.23 (d, 1, J = 6, H-16), 4.52 (AB q, 2, $\Delta\nu$ = 0.52 ppm, J = 20, H-21), 1.55 (s, 3, ketal CH_3), 0.69 (s, 3, 18-CH_3); ^{13}C NMR δ 210.4, 199.7, 165.9, 152.9, 142.7, 124.7, 110.1, 107.5, 98.0, 82.8, 67.2, 48.9, 47.9, 46.9, 42.2, 39.4, 36.4, 35.2, 33.4, 31.4, 31.1, 26.4, 25.6, 24.3, 14.8; IR ($CHCl_3$) 1705, 1670, 1120, 1280, 1170, 1095 cm^{-1}; mp

198–200 °C; HPLC t_R 35 min; HRMS (CI, M + H) calcd for $C_{26}H_{33}O_6$ 441.2277, found 441.2273. Anal. ($C_{26}H_{32}O_6{}^1/_2H_2O$) C, H.

Data for exo-8b: ^{1}H NMR δ 7.34 (d, 1, J = 2), 6.25 (d, 1, J = 3), 6.17 (d, 1, J = 3), 5.86 (br s, 1, H-4), 5.26 (d, 1, J = 5, H-16), 3.90 (AB q, 2, Δν = 0.073 ppm, J = 20, H-21), 1.78 (s, 3, ketal CH_3), 0.64 (s, 3, 18-CH_3); ^{13}C NMR δ 209.8, 199.8, 165.8, 153.3, 142.5, 124.8, 110.3, 108.1, 106.7, 97.7, 84.6, 66.8, 48.8, 48.3, 47.0, 42.3, 39.5, 36.5, 35.3, 33.8, 31.4, 31.2, 26.5, 25.8, 24.3, 14.9; IR ($CHCl_3$) 1705, 1670, 1120, 1280, 1170, 1095 cm^{-1}; mp 218–220 °C; HPLC t_R 50 min; HRMS (CI, M + H) calcd for $C_{26}H_{33}O_6$ 441.2277, found 441.2270.

16α,17α-[(*R*)-(1′-α-Furylmethylidene)dioxy]-21-[[(trifluoromethyl)sulfonyl]oxy]-19-norpregn-4-ene-3,20-dione (endo-9a). To endo-**8a** (9 mg, 0.021 mmol) in 0.5 mL of CH_2Cl_2 at −78 °C were added 2,6-lutidine (2.9 mg, 0.027 mmol) and triflic anhydride (6.5 mg, 0.023 mmol). After 0.5 h, the reaction was quenched at −78 °C with MeOH, the solution was warmed to 0 °C, and water was added. Product isolation followed by flash chromatography (10:1 hexanes/EtOAc) afforded 4 mg (34%) of endo-**9a:** ^{1}H NMR δ 7.49 (br s, 1), 6.55 (d, 1, J = 3), 6.41 (d, 1, J = 3), 5.86 (br s, 1, H-4), 5.63 (s, 1, acetal H), 5.26 (AB q, 2, Δν = 0.30 ppm, J = 18, H-21), 5.07 (d, 1, J = 5.6, H-16), 0.79 (s, 3, 18-CH_3); ^{13}C NMR δ 199.3, 199.6, 165.5, 147.8, 143.9, 124.9, 110.4 (2C), 98.3, 98.1, 83.1, 76.3, 48.6, 47.9, 47.2, 42.2, 39.4, 36.4, 35.2, 33.2, 31.5, 31.0, 26.5, 25.6, 14.7 (trifluoromethyl carbon unobservable); mp 115–116 °C dec; HRMS (CI, M + H) calcd for $C_{26}H_{30}O_8SF_3$ 559.1614, found 559.1602.

16α,17α-[(*S*)-(1′-β-Furylmethylidene)dioxy]-21-[[(trifluoromethyl)sulfonyl]oxy]-19-norpregn-4-ene-3,20-dione (exo-9a). To exo-**8a** (19 mg, 0.045 mmol) and 2,6-lutidine (6 mg, 0.058 mmol) in 1 mL of CH_2Cl_2 at −78 °C was added triflic anhydride (15 mg, 0.053 mmol) over 10 min. After 0.5 h, the reaction was quenched at −78 °C with MeOH, the solution was warmed to 0 °C, and water was added. Product isolation followed by flash chromatography (5:1 hexanes/EtOAc) afforded 15 mg (60%) of exo-**9a:** ^{1}H NMR δ 7.43 (br s, 1), 6.41 (d, 1, J = 3), 6.37 (d, 1, J = 3), 6.19 (s, 1, acetal H), 5.86 (br s, 1, H-4), 5.30 (d, 1, J = 6, H-16), 5.01 (AB q, 2, Δν = 0.09 ppm, J = 17, H-21), 0.81 (s, 3, 18-CH_3); ^{13}C NMR δ 199.7, 198.8, 165.4, 149.6, 143.6, 124.9, 110.6, 110.4, 100.3, 98.2, 84.8, 76.8, 49.5, 48.7, 48.2, 42.2, 39.7, 36.4, 35.2, 33.0, 31.5, 31.1, 26.5, 25.6, 14.9 (trifluoromethyl carbon unobservable).

16α,17α-[(*R*)-(1′-α-Furylethylidene)dioxy]-21-[[(trifluoromethyl)sulfonyl]oxy-19-norpregn-4-ene-3,20-dione (endo-9b). To endo-**8b** (20 mg, 0.045 mmol) and 2,6-lutidine (6 mg, 0.058 mmol) in 1 mL of CH_2Cl_2 at −78 °C was added triflic anhydride (15 mg, 0.053 mmol) over 10 min. After 0.25 h, the reaction was quenched at −78 °C with MeOH, the solution was warmed to 0 °C, and water was added. Product isolation followed by flash chromatography (5:1 hexanes/EtOAc) afforded 19 mg (73%) of **endo-9b:** ^{1}H NMR δ 7.43 (br s, 1), 6.43 (d, 1, J = 3), 6.37 (d, 1, J = 3), 5.85 (br s, 1, H-4), 5.30 (AB q, 2, Δν = 0.50 ppm, J = 18, H-21), 5.24 (d, 1, J = 5.6, H-16), 1.61 (s, 3, ketal CH_3), 0.75 (s, 3, 18-CH_3); ^{13}C NMR δ 199.6 (2C), 165.5, 152.5, 142.9, 124.9, 110.2, 108.1, 107.6, 98.2, 83.2, 76.3, 48.8, 47.9, 47.1, 42.2, 39.4, 36.5, 35.2, 33.4, 31.6, 31.1, 26.5, 25.6, 24.4, 14.8 (trifluoromethyl carbon unobservable); mp 135–137 °C dec; HRMS (CI, M + H) calcd for $C_{27}H_{32}O_8SF_3$ 573.1770, found 573.1753.

21-Fluoro-16α,17α-[(*R*)-(1′-α-furylmethylidene)dioxy]-19-norpregn-4-ene-3,20-dione (endo-10a) and 21-Fluoro-16α,17α-[(*S*)-(1′-β-furylmethylidene)dioxy]-19-norpregn-4-ene-3,20-dione (exo-10a). To a 3:1 mixture of exo-**9a** and endo-**9a** (40 mg, 0.075 mmol) in THF at 0 °C was added n-Bu_4NF (90 μL of 1.0 M in THF, 0.090 mmol) over 10 min. After 45 min, product isolation followed by flash chromatography (10:1 hexanes/EtOAc) afforded 14 mg (44%) of a 3:1 mixture of exo-**10a** and endo-**10a.** Semipreparative HPLC (60/40 water/CH_3CN, 5 mL/min) afforded analytical samples for characterizatioin and binding affinity measurements.

Data for endo-10a: ^{1}H NMR δ 7.48 (d, 1, J = 2), 6.53 (d, 1, J = 3), 6.40 (d, 1, J = 3), 5.86 (br s, 1, H-4), 5.62 (s, 1, acetal H), 5.21 (d, J_{HF} = 47, AB q, 2, Δν = 0.24 ppm, J_{HH} = 17, H-21), 0.78 (s, 3, 18-CH_3); ^{19}F NMR φ −234.1 (t, J = 46); IR ($CHCl_3$) 1740, 1670, 1610, 1100 cm^{-1}; mp 173–175 °C; HPLC t_R 21 min; HRMS (CI, M + H) calcd for $C_{25}H_{30}O_5F$ 429.2077, found 429.2068.

Data for exo-10a: ^{1}H NMR δ 7.42 (d, 1, J = 2), 6.38–6.34 (m, 2), 6.19 (s, 3, acetal H), 5.86 (br s, 1, H-4), 5.31 (d, 2, J_{HF} = 46, H-21), 0.80 (s, 3, 18-CH_3); ^{19}F NMR φ −233.7 (t, J = 46); IR ($CHCl_3$) 1740, 1670, 1610, 1100 cm^{-1}; mp 171–172 °C; HPLC t_R 25 min; HRMS (CI, M + H) calcd for $C_{25}H_{30}O_5F$ 429.2077, found 429.2068.

21-Fluoro-16α,17α-[(*R*)-(1′-α-furylethylidene)dioxy]-19-norpregn-4-ene-3,20-dione (endo-10b). To a solution of endo-**9b** (13 mg, 0.023 mmol) in THF at 0 °C was added n-Bu_4NF (30 μL of 1.0 M in THF, 0.030 mmol) over 5 min. After 50 min, product isolation followed by flash chromatography (10:1 hexanes/EtOAc) afforded 3 mg (25%) of endo-**10b.** Semipreparative HPLC (50/50 water/CH_3CN, 5 mL/min) afforded analytical samples for characterization and binding affinity measurements: ^{1}H NMR δ 7.42 (d, 1, J = 2), 6.43 (d, 1, J = 3), 6.37 (m, 1), 5.85 (br s, 1, H-4), 5.23 (d, 1, J = 6, H-16), 5.22 (d, J_{HF} = 47, AB q, 2, Δν = 0.39 ppm, J_{HH} = 17, H-21), 1.59 (s, 3, ketal CH_3), 0.74 (s, 3, 18-CH_3); ^{19}F NMR φ −233.7 (t, J = 46); IR ($CHCl_3$) 1740, 1670, 1610, 1100 cm^{-1}; HPLC t_R 10 min; HRMS (CI, M + H) calcd for $C_{26}H_{32}O_5F$ 443.2233, found 443.2215.

Radiochemical Synthesis. General. Fluorine-18 was produced by the ^{18}O(p,n)^{18}F reaction on an enriched water target.[23] Oxygen-18 water containing the ^{18}F anion was transferred to a Vacutainer containing n-Bu_4NOH (1 M in water, 2.3 μL, 2.3 μmol). The water was removed azeotropically under a gentle stream of nitrogen with the continuous addition of 0.5–1.5 mL of acetonitrile at 110 °C (oil bath). Before being completely dried, the Vacutainer was removed from the oil bath and the final drying process was completed by the gentle stream of nitrogen at room temperature.[24] The resolubilized [^{18}F]fluoride ion was dissolved in 300 μL of freshly distilled THF and transferred to a glass vial containing 1.5 mg of the desired 21-triflate substrates endo-**9a** or endo-**9b.** The resolubilization procedure took 10–15 min with 85–95% of the initial activity being recovered. After 5–7 min, the reaction mixture was passed through a SiO_2 plug (5 mm × 5 mm) with THF. n-Bu_4NOH (1 M in water, 6.75 μL, 6.75 μmol) was added to the eluent to destroy excess unreacted trifate. After 2 min at 25 °C, the reaction mixture was passed through another SiO_2 plug (5 mm × 5 mm) with THF and evaporated in vacuo. The residue was dissolved in 85:15 CH_2Cl_2/hexanes and purified by semipreparative HPLC (Whatman M9/50 silica gel, 85% hexanes, 15% 20:1 CH_2Cl_2/i-PrOH, 5 mL/min). Eluent was monitored by UV detection at 254 nm and a NaI(Tl) radioactivity detector. End of synthesis yields are based on resolubilized activity and are decay corrected. Effective specific activities were measured by in vitro competitive binding assays preformed on fully decayed samples.[20] Radioactivity was measured in a well counter.

21-[*Fluoro*-^{18}F]-16α,17α-[(*R*)-(1′-α-furylmethylidene)-dioxy]-19-norpregn-4-ene-3,20-dione ([^{18}F]endo-10a): yield range 2–13%; t_R 35.4 min; effective specific activity = 1239 Ci/mmol.

21-[*Fluoro*-^{18}F]-16α,17α-[(*R*)-(1′-α-furylethylidene)dioxy]-19-norpregn-4-ene-3,20-dione ([^{18}F]endo-10b): yield range 3–8%; t_R 34.3 min; effective specific activity = 1476 Ci/mmol.

Biological Procedures. Measurement of Relative Receptor Binding Affinity. Progesterone RBA's were determined using competitive radiometric binding assays using a tritium-labeled R5020 standard.[7c] By definition, the standard has an RBA value of 100.

In Vivo Tissue Biodistribution Studies. PR levels in the uteri of immature female Sprague–Dawley rats (25 days old, ≈50 g, five rats per time point) were induced by daily sc injections for 2 days of 5 μg of estradiol in 0.1 mL of 50% ethanol/sunflower seed oil. The experiments were begun 24 h after the last injection. The ^{18}F-labeled progestins, purified by HPLC, were concentrated in vacuo, redissoved in ≈0.60 mL of ethanol and ≈6.0 mL of isotonic saline, and passed through a filter (0.45 μm). Anesthetized rats were injected in the tail vein with 12–70 μCi of the labeled compound. Normal doses employed were 70 μCi in 250 μL of 10% ethanol/saline per rat

for [^{18}F]endo-**10a** and 60 μCi in 250 μL of 10% ethanol/saline per rat for [^{18}F]endo-**10b**. At the specified time points postinjection, the rats were sacrificed by decapitation and blood and organs were removed, weighed, and counted in a Beckman Gamma 6000 counter. To determine whether the uptake was mediated by a high-affinity, limited-capacity system, one set of animals was coinjected with the fluorine-18-labeled progestin together with 18 μg of ORG 2058 in order to fully occupy the progesterone receptors (Tables 2 and 3, 1 h "blocked"). To establish that the uptake was not being limited by undetected PR binding impurities, one set of animals was injected with only 20% of the 1 h dose (Tables 2 and 3, 1 h "low dose").

Acknowledgment. We are grateful for support of this work through grants from the Department of Energy (DE FG02 86ER 60401 to J.A.K. and DE FG02-84ER60218 to M.J.W.) and the National Institutes of Health (PHS 5R01 HL13851 to M.J.W.). High-resolution mass spectra were obtained on a VG 70-VSE supported by grants from the National Institutes of Health to the University of Illinois (RR 04648). We thank Kathryn E. Carlson, Kathy Tongue, Anita M. Skariah, Karen Avenatti, and Elizabeth L. C. Sherman for their helpful assistance.

Supplementary Material Available: Analytical data and HPLC traces of compounds endo/exo-**8a**, **8b**, **9a**, **10a**, endo-**9b**, and **10b** (11 pages). Ordering information is given on any current masthead page.

References

(1) (a) Ganz, P. A.; Korenman, S. G. The Clinical Value of Steroid Receptors in Breast Cancer. In *Cancer Diagnosis: New Concepts and Techniques*; Steckle, R. J., Kagan, A. R., Eds.; Grune & Stratton: New York, 1982; pp 32–61. (b) Sledge, G. W., Jr.; McGuire, W. L. Steroid Hormone Receptors in Human Breast Cancer. *Adv. Cancer Res.* **1983**, *38*, 61–75. (c) Horowitz, K. B. The Structure and Function of Progesterone Receptors in Breast Cancer. *J. Steroid Biochem.* **1987**, *27*, 447–457. (d) McGuire, W. L. Steroid Hormone Receptors and Deisease: Breast Cancer. *Proc. Soc. Exp. Biol. Med.* **1979**, *162*, 22–25. (e) Gelbfish, G. A.; Davison, A. L.; Kopel, S.; Schreibmen, B.; Gelbfish, J. S.; Degenshein, G. A.; Herz, E. L.; Cunningham, J. N. Relationship of Estrogen and Progesterone Receptors to Prognosis in Breast Cancer. *Ann. Surg.* **1988**, *207*, 75–79.

(2) Furr, B. J. A.; Jordan, V. C. The Pharmacology and Clinical Uses of Tamoxifen. *Pharmacol. Ther.* **1984**, *25*, 127.

(3) (a) Noguchi, S.; Miyauchi, K.; Nishizawa, Y.; Koyama, H. Induction of Progesterone Receptor with Tamoxifen in Human Breast Cancer with Special Reference to its Behavior over Time. *Cancer* **1988**, *61*, 1345–1349. (b) Howell, A.; Harland, R. N. L.; Barnes, D. M.; Baildam, A. D.; Wilkinson, M. J. S.; Hayward, E.; Swindell, R.; Sellwood, R. A. Endocrine Therapy for Advanced Carcinoma of the Breast: Relationship Between the Effect of Tamoxifen upon Concentrations of Progesterone Receptor and Subsequent Response to Treatment. *Cancer Res.* **1987**, *47*, 300–304. (c) Namer, M.; Lalanne, C.; Baulieu, E. Increase of Progesterone Receptor by Tamoxifen as a Hormonal Challenge Test in Breast Cancer. *Cancer Res.* **1980**, *40*, 1750.

(4) For a review, see: Katzenellenbogen, J. A. The Pharmacology of Steroid Radiopharmaceuticals: Specific and Non-specific Binding and Uptake Selectivity. In *Radiopharmaceuticals: Chemistry and Pharmacology*; Nunn, A., Ed.; Marcel Dekker: New York, 1992; pp 297–331.

(5) VanBrocklin, H. F.; Carlson, K. E.; Katzenellenbogen, J. A.; Welch, M. J. 16β-([^{18}F]Fluoro)estrogens: Systematic Investigation of a New Series of Fluorine-18-Labeled Estrogens as Potential Imaging Agents for Estrogen-Receptor-Positive Breast Tumors. *J. Med Chem.* **1993**, *36*, 1619–1629 and references cited therein.

(6) (a) Mintun, M. A.; Welch, M. J.; Siegel, B. A.; Mathias, C. J.; Brodack, J. M.; McGuire, A. H.; Katzenellenbogen, J. A. Breast Cancer: PET Imaging of Estrogen Receptors. *Radiology* **1988**, *169*, 45–48. (b) McGuire, A. H.; Dedashti, F.; Siegel, B. A.; Lyss, A. P.; Brodack, J. W.; Mathias, C. J.; Mintun, M. A.; Katzenellenbogen, J. A.; Welch, M. J. Positron Tomagraphic Assessment of 16α-[^{18}F]Fluoro-17β-Estrodiol Uptake in Metastatic Breast Carcinoma. *J. Nucl. Med.* **1991**, *32*, 1526–1531. (c) Preston, D. F.; Spicer, J. A.; Baranczuk, R. A.; Jewell, W. R.; Krishnan, L.; Wegst, A. V.; Robinson, G. In Vivo Imaging of Estrogen Receptors by Extremely High Specific Activity 16 Alpha I-123 Iodoestradiol-17 Beta. *Radiology* **1986**, *161*, 403. (d) Scheidhauer, K.; Muller, S.; Smolarz, K.; Brautigam, P.; Briele, B. Tumor-Szintigraphie mit ^{123}J-Markiertem Östradiol beim Mammakarzinom-Rezeptorszintigraphie. (Tumor Scintigraphy using I-123 Labeled Estradiol in Breast-Cancer-Receptor Scintigraphy.) *NuklearMedizin* **1991**, *30*, 84–99. (e) Ribeiro-Barras, M.; Coulon, C.; Baulieu, J.; Guilloteau, D.; Bougnoux, P.; Lansac, J.; Besnard, J. Estrogen Receptor Imaging with 17α-[123I]iodovinyl-11β-methoxyestradiol (MIVE2)—Part II. Preliminary Results in Patients with Breast Carcinoma. *Nucl. Med. Biol.* **1992**, *19*, 263–267. (f) Kenady, D.; Pavlik, E.; Nelson, K.; van Nagell, F.; Gallion, H.; DePriest, P.; Ryo, U.; Baranczuk, R. Images of Estrogen-Receptor-Positive Breast Tumors Produced by Estradiol Labeled Iodine I-123 at 15 Alpha. *Arch. Surg.* **1993**, *128*, 1373–1381.

(7) (a) Pomper, M. G.; Katzenellenbogen, J. A.; Welch, M. J.; Brodack, J. W.; Mathias, C. J. 21-[^{18}F]Fluoro-16α-ethyl-19-norprogesterone: Synthesis and Target Tissue Selective Uptake of a Progestin Receptor Based Radiotracer for Positron Emission Tomography. *J. Med. Chem.* **1988**, *31*, 1360–1363. (b) Carlson, K. E.; Brandes, S. J.; Pomper, M. G.; Katzenellenbogen, J. A. Uptake of Three [^{3}H]Progestins by Target Tissues In Vivo: Implications for the Design of Diagnostic Imaging Agents. *Nucl. Med. Biol.* **1988**, *15*, 403–408. (c) Brandes, S. J.; Katzenellenbogen, J. A. Fluorinated Androgens and Progestins: Molecular Probes for Androgen and Progesterone Receptors with Potential Use in Positron Emission Tomography. *Mol. Pharmacol.* **1987**, *32*, 391–403. (d) Brandes, S. J.; Katzenellenbogen, J. A. Fundamental Considerations in the Design of Fluorine-18 Labeled Progestins and Androgens as Imaging Agents for Receptor-Positive Tumors of the Breast and Prostate. *Nucl. Med. Biol.* **1988**, *15*, 53–67. (e) Pomper, M. G.; Pinney, K. G.; Carlson, K. E.; VanBrocklin, H.; Mathias, C. J.; Welch, M. J.; Katzenellenbogen, J. A. Target Tissue Uptake Selectivity of Three Fluorine-substituted Progestins: Potential Imaging Agents for Receptor-positive Breast Tumors. *Nucl. Med. Biol.* **1990**, *17*, 309–319. (f) De Groot, T. Synthesis & Evaluation of [^{18}F]Fluoroprogestins and [^{18}F]Fluorometoprolol. Ph.D. Thesis, University of Groningen, The Netherlands, 1993. (g) Spitznagle, L. A.; Kasina, S.; Marino, C. A. Design of Radiopharmaceuticals for Structure Distribution Studies: Some Fluorine-18 Labeled Pregnane Derivatives. *Nucl. Med. Biol. Adv.*; Proc. World Congr., 3rd, 1982; 1983; Vol. 1, pp 636–639. (h) Hoyte, R. M.; Rosner, W.; Johnson, I. S.; Zielinski, J.; Hochberg, R. B. Synthesis and Evaluation of Potential Radioligands for the Progesterone Receptor. *J. Med. Chem.* **1985**, *28*, 1695–1699.

(8) (a) Dedashti, F.; McGuire, A. M.; VanBrocklin, H. F.; Siegel, B. A.; Andriole, D. P; Griffeth, L. K.; Pomper, M. G.; Katzenellenbogen, J. A.; Welch, M. J. Assessment of 21-[^{18}F]Fluoro-16α-Ethyl-19-Norprogesterone as a Positron-Emitting Radiopharmaceutical for the Detection of Porgestin Receptors in Human Breast Carcinomas. *J. Nucl. Med.* **1991**, *32*, 1532–1537. (b) Verhagen, A.; Studeny, M.; Luurtsema, G.; Vissar, G. M.; de Goeij, C. C. J.; Sluyser, M.; Nieweg, O. E.; Van der Ploeg, E.; Go, K. G.; Vaalburg, W. Metabolism of a [^{18}F]Fluorine Labeled Progestin (21-[^{18}F]Fluoro-16α-ethyl-19-norprogesterone) in Humans: a Clue for Future Investigations. *Nucl. Med. Biol.* **194**, *21*, 941–952.

(9) Kochanny, M. J.; VanBrocklin, H. F.; Kym, P. R.; Carlson, K. E.; O'Neil, J. P.; Bonasera, T. A.; Welch, M. J.; Katzenellenbogen, J. A. Fluorine-18-Labeled Progestin Ketals: Synthesis and Target Tissue Uptake Selectivity of Potential Imaging Agents for Receptor-Positive Breast Tumors. *J. Med. Chem.* **1993**, *36*, 1120–1127.

(10) Cooke, B. A.; Vallance, D. K. Metabolism of Megestrol Acetate and Related Progesterone Analogues by Liver Preparations in vitro. *Biochem. J.* **1965**, *97*, 672–677.

(11) (a) Kym, P. R.; Carlson, K. E.; Katzenellenbogen, J. A. Progestin 16α,17α-Dioxolane Ketals as Molecular Probes for the Progesterone Receptor: Synthesis, Binding Affinity, and Photochemical Evaluation. *J. Med. Chem.* **1993**, *36*, 1111–1119. (b) Kochanny, M. J. Fluorine-18 labeled Corticosteroids and Progestins for Receptor-Based Imaging of the Brain and of Breast Tumors. Synthesis and NMR Spectrum of (^{13}C$_{18}$)-*meso*-Hexestrol. Ph.D. Thesis, University of Illinois, Urbana, IL, 1993.

(12) (a) Fried, J.; Sabo, E. F.; Grabowich, P.; Lerner, L. J.; Kessler, W. B.; Brennan, D. M.; Borman, A. Progestationally Active Acetals and Ketals of 16α,17α-Dihydroxyprogesterone. *Chem. Ind.* **1961**, 465–466. (b) Fried, J.; Sabo, E. F. The Stereochemistry of Unsymmetrically Substituted 16α,17α-Methylenedioxyprogesterones. In *Hormonal Steroids, Biochemistry, Pharmacology and Therapeutics: Proceedings of the First International Congress on Hormonal Steroids*; Academic Press: New York, 1965; Vol. 2, pp 15–21.

(13) Wieland, P. Neue Verfahren zur Herstellung von 21-Fluorosteroiden. (Steroids. 232. New Methods for Preparation of 21-Fluoro-Steroids.) *Helv. Chem. Acta* **1976**, *59*, 1027–1034.

(14) Kilbourn, M. R. *Fluorine-18 Labeling of Radiopharmaceuticals*; National Academy Press: Washington, DC, 1990.
(15) (a) Spitznagle, L. A.; Marino, C. A. Synthesis of Fluorine-18 Labeled 21-Fluoroprogesterone. *Steroids* **1977**, *30*, 435–438. (b) Pomper, M. G.; Kochanny, M. J.; Thieme, A. M.; Carlson, K. E.; VanBrocklin, H. F.; Mathias, C. J.; Welch, M. J.; Katzenellenbogen, J. A. *Nucl. Med. Biol.* **1992**, *19*, 461–480.
(16) (a) Lerner, L. J.; Brennan, D. M.; Borman, A. Biological Activities of 16α,17α-Dihydroxyprogesterone Derivatives. *Proc. Soc. Exp. Biol. Med.* **1961**, *106*, 231–234. (b) Seeley, D. H.; Wang, W.-Y.; Salhanick, H. A. Molecular Interactions of Progesterone Analogues with Rabbit Uterine Cytoplasmic Receptor. *J. Biol. Chem.* **1982**, *257*, 13359–13366.
(17) Katzenellenbogen, J. A.; Heiman, D. F.; Carlson, K. E.; Lloyd, J. E. In vivo and in vitro Steroid Receptor Assays in the Design of Estrogen Radiophamaceuticals. In *Receptor-Binding Radiotracers*; Eckelman, W. C., Ed.; CRC: Boca Raton, FL, 1982; Vol. 1, pp 93–126.
(18) Minick, D. J.; Frenz, J. H.; Patrick, M. A.; Brent, D. A. A Comprehensive Method for Determining Hydrophobicity Constants by Reversed-Phase High-Performance Liquid Chromatography. *J. Med. Chem.* **1988**, *31*, 1923–1933.
(19) Rekker, R. F.; Mannhold, R. *Calculation of Drug Lipophilicity*; VCH: Weinheim, Germany, 1992.
(20) Senderhoff, S. G.; McElvany, K. D.; Carlson, K. E.; Heiman, D. F.; Katzenellenbogen, J. A.; Welch, M. J. Methodology for the Synthesis and Specific Activity Determination of 16α-[^{77}Br]-Bromoestradiol-17β and 16α-[^{77}Br]Bromo-11β-methoxyestradiol-17β, Two Estrogen Receptor-Binding Radiopharmaceuticls. *Int. J. Appl. Radiat. Isot.* **1982**, *33*, 454–551.
(21) Weisman, R. A.; Sahakian, J. A.; Brodack, J. W.; Welch, M. J.; Merrill, J. C.; Li, A. P.; Katzenellenbogen, J. A. The Use of Cultured Liver Cells from Rats and Humans to Study the Metabolism of the PET Imaging Agent (^{18}F)-Fluoroestradiol [Abstract]. *J. Labelled Compd. Radiopharm.* **1991**, *30*, 426.
(22) Still, W. C.; Kahn, M.; Mitra, A. A Rapid Chromatagraphic Technique for Preparative Separations with Moderate Resolution. *J. Org. Chem.* **1978**, *43*, 2923–2925.
(23) Kilbourn, M. R.; Jerabek, P. A.; Welch, M. J. An Improved [^{18}O]-Water Target for [^{18}F]Fluoride Production. *Int. J. Appl. Radiat. Isot.* **1985**, *36*, 327–328.
(24) Brodack, J. W.; Kilbourn, M. R.; Welch, M. J.; Katzenellenbogen, J. A. NCA 16α-[^{18}F]Fluoroestradiol-17β: The Effect of Reaction Vessel on Fluorine-18 Resolubilization, Product Yield, and Effective Specific Activity. *Appl. Radiat. Isot.* **1986**, *37*, 217–221.

JM940551Y